

A Cytoplasmically Inherited Barley Mutant Is Defective in Photosystem I Assembly Due to a Temperature-Sensitive Defect in *ycf3* Splicing^{1[W]}

Alejandra Mabel Landau*, Heiko Lokstein, Henrik Vibe Scheller, Verónica Lainez, Sara Maldonado, and Alberto Raúl Prina

Instituto de Genética E.A. Favret, Centro de Investigaciones en Ciencias Veterinarias y Agronómicas, Instituto Nacional de Tecnología Agropecuaria, B1712WAA Castelar, Province of Buenos Aires, Argentina (A.M.L., A.R.P.); Institut für Biochemie und Biologie, Universität Potsdam, D-14476 Potsdam-Golm, Germany (H.L.); Department of Plant Biology and Biotechnology, University of Copenhagen, DK-1871 Frederiksberg C, Denmark (H.V.S.); Joint Bioenergy Institute, Emeryville, California 94608 (H.V.S.); Consejo Nacional de Investigaciones Científicas y Técnicas, Departamento de Biodiversidad y Biología Experimental, Facultad de Ciencias Exactas y Naturales, Universidad de Buenos Aires, C1428EGA Buenos Aires, Argentina (V.L., S.M.); and Instituto de Recursos Biológicos, Centro de Investigación de Recursos Naturales, Instituto Nacional de Tecnología Agropecuaria, B1712WAA Castelar, Province of Buenos Aires, Argentina (S.M.)

A cytoplasmically inherited chlorophyll-deficient mutant of barley (*Hordeum vulgare*) termed cytoplasmic line 3 (CL3), displaying a *viridis* (homogeneously light-green colored) phenotype, has been previously shown to be affected by elevated temperatures. In this article, biochemical, biophysical, and molecular approaches were used to study the CL3 mutant under different temperature and light conditions. The results lead to the conclusion that an impaired assembly of photosystem I (PSI) under higher temperatures and certain light conditions is the primary cause of the CL3 phenotype. Compromised splicing of *ycf3* transcripts, particularly at elevated temperature, resulting from a mutation in a noncoding region (intron 1) in the mutant *ycf3* gene results in a defective synthesis of Ycf3, which is a chaperone involved in PSI assembly. The defective PSI assembly causes severe photoinhibition and degradation of PSII.

Chlorophyll (Chl)-deficient mutants have been extensively utilized to study development and functions of chloroplasts (e.g. Gustafsson, 1942; Von Wettstein, 1961; Taylor et al., 1987; Von Wettstein et al., 1995; Leon et al., 1998). Most of the Chl-deficient mutants reported previously originate from nuclear gene mutations. This is not surprising since most of the genes necessary for plastid development and pigment biosynthesis have migrated from plastids to the nucleus during

evolution of plants (Hess and Börner, 1999). Previously, some cytoplasmically inherited Chl-deficient mutants selected from a family carrying a mutator genotype in barley (*Hordeum vulgare*) have been described (Prina, 1992, 1996). Mutants viable under field conditions have been selected to facilitate their multiplication, hybridization, and, later on, selection of nonmutator type, genetically stable genotypes. Due to their breeding behavior, those mutants were called cytoplasmic lines (CLs; Prina, 1996). One of these lines, termed CL3, exhibits a *viridis* (homogeneously light-green colored) phenotype, which is much more pronounced at elevated temperatures (Prina et al., 1996). Wild-type barley seedlings become chlorotic at growth temperatures in excess of 32°C (Smillie et al., 1978). Some temperature-sensitive mutants, which were previously described, showed heat sensitivity for chloroplast development at temperatures lower than those producing chlorosis in wild type and also, a decrease of PSI and PSII activities (Smillie et al., 1978). In all these mutants, the genes affected were nuclear encoded. Hence, CL3 is the first temperature-sensitive chloroplast gene mutant described in higher plants. Chlorosis is a syndrome that can result from primary deficiencies at many different points in the chloroplasts. Not surprisingly, mutants in Chl biosynthesis are chlorotic, but so are mutants, for example, in

¹ This work was supported by Instituto Nacional de Tecnología Agropecuaria and Proyecto de Investigación Científica y Técnica (no. 04841), Agencia Nacional de Promoción Científica y Tecnológica, Argentina; the U.S. Department of Energy, Office of Science, Office of Biological and Environmental Research (through contract no. DE-AC02-05CH11231 between Lawrence Berkeley National Laboratory and the U.S. Department of Energy); and the Danish National Research Foundation. H.L. acknowledges financial support by the Deutsche Forschungsgemeinschaft (grant no. SFB 429, TP A2).

* Corresponding author; e-mail alandau@cnia.inta.gov.ar.

The author responsible for distribution of materials integral to the findings presented in this article in accordance with the policy described in the Instructions for Authors (www.plantphysiol.org) is: Alejandra Mabel Landau (alandau@cnia.inta.gov.ar).

^[W] The online version of this article contains Web-only data.

www.plantphysiol.org/cgi/doi/10.1104/pp.109.147843

carotenoid biosynthesis or in the function of either of the photosystems. In the latter cases, chlorosis is primarily a result of reactive oxygen species that are generated as a result of inefficient radical scavenging or due to faulty electron transfer processes. Since reactive oxygen species cause damage to many chloroplast components, a primary mutation at any point of the electron transport chain can cause damage to other sites of the chain and to pigment biosynthesis, thereby causing generation of even more reactive oxygen and exacerbated damage. Hence, it can be difficult to determine the primary cause of chlorotic phenotypes.

In this article, biochemical, biophysical, and molecular approaches were used to study the responses of the CL3 mutant to different temperatures and light conditions. The results show that an impaired assembly of PSI causes the CL3 phenotype and results in photodamage to the entire photosynthetic apparatus. Compromised and temperature-dependent splicing of *ycf3* transcripts resulting from a mutated noncoding region (intron 1) in *ycf3* is the primary cause of the phenotype.

RESULTS

The *viridis* Phenotype of the CL3 Mutant Is More Pronounced at Higher Temperatures

Figure 1 shows wild-type and CL3 barley seedlings growing at two different temperatures and light qualities 6 d after germination. The permissive and optimal temperature was chosen at 18°C and 32°C as the restricted temperature for stress treatment. The light environments were provided by either a combination of fluorescent and incandescent light or solely by fluorescent light, at 100 $\mu\text{mol photons m}^{-2} \text{s}^{-1}$ in both growth chambers. At 18°C the mutant showed a slightly pale phenotype (Fig. 1, A and C), which was more pronounced in fluorescent light than in the combination of fluorescent and incandescent light. At 18°C the CL3 plants would develop and set seeds in spite of the mutation. At 32°C the *viridis* phenotype of CL3 was much more pronounced, and none of the plants survived (Fig. 1, B and C), but again the phenotype was much more severe in fluorescent light (Fig. 1D) than in the combination light (Fig. 1B).

Unless otherwise noted, all experiments reported below were carried out with seedlings 6 d after germination, grown in the mixed light, i.e. plants corresponding to Figure 1, A and B.

Pigment Contents

To quantify Chl content and to investigate to what extent the contents of other pigments were altered, barley seedlings were grown for 6 d after germination at the two temperatures mentioned above under a combination of fluorescent and incandescent light, and pigments were quantified by HPLC (Table I). Chl content was slightly reduced in wild-type leaves at

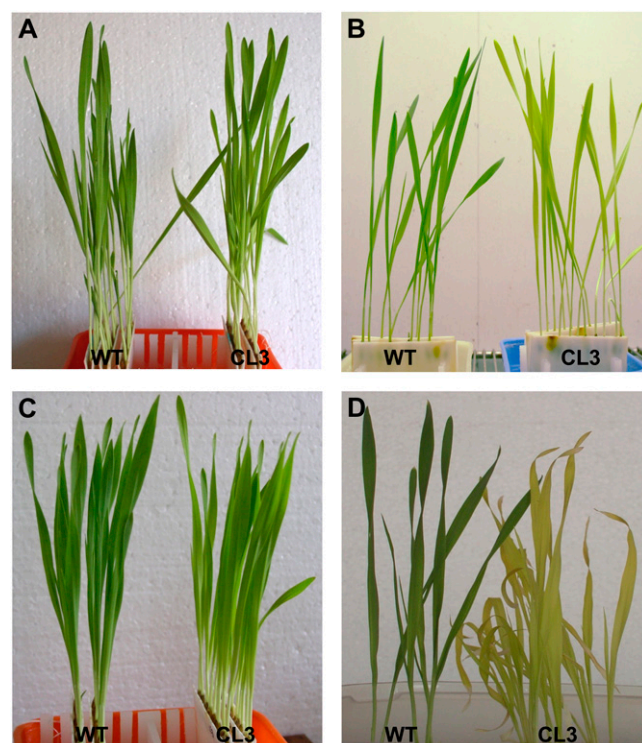


Figure 1. Wild-type (WT) and CL3 mutant barley seedlings 6 d after germination in different light quality (100 $\mu\text{mol photons m}^{-2} \text{s}^{-1}$) and temperature environments. A, 18°C under a mixture of fluorescent and incandescent light. B, 32°C under a mixture of fluorescent and incandescent light. C, 18°C under fluorescent light only. D, 32°C under fluorescent light only.

32°C and the CL3 mutant grown at 18°C as compared to wild type at 18°C, but reduced to about 24% of wild-type levels in the mutant at 32°C.

Xanthophyll-cycle pigments (violaxanthin [V], antheraxanthin [A], and zeaxanthin [Z], determined relative to Chl) were increased 2-fold in CL3 compared to wild type at both temperatures. Temperature did not have a significant effect on the VAZ-to-Chl ratio. However, the deepoxidation state of V + A + Z was increased in CL3 already at 18°C, and at 32°C more than 50% of the xanthophyll cycle pigment pool was partially or completely deepoxidated.

Effects of Growth Temperature on Chloroplast Ultrastructure in the CL3 Mutant

Transmission electron microscopy revealed striking differences in the ultrastructure of plastids from CL3 plants grown at 32°C as compared to those grown at 18°C under fluorescent light only (Fig. 2, A–D). In the mutant, at 32°C mesophyll cells had small plastids of abnormal appearance, with a rather elongated shape containing clumps of electron-dense material as well as an increased number of plastoglobuli. Numerous thylakoids and grana-like structures with swollen thylakoids were found in most of the plastids (Fig. 2, A and B).

Table 1. Pigment contents and composition in barley 6 d after germination

Wild-type and CL3 mutant leaves grown at 100 $\mu\text{mol photons m}^{-2} \text{s}^{-1}$ under a mixture of fluorescent and incandescent light at different temperatures. The data are the means of at least 15 measurements (\pm SD).

Samples	Chl <i>a+b</i> $\mu\text{g/cm}^2$	VAZ $\mu\text{g/cm}^2$	Z + 0.5A/VAZ	Neoxanthin $\mu\text{g/cm}^2$	Lutein $\mu\text{g/cm}^2$	β -Carotene $\mu\text{g/cm}^2$
Wild type 18°C	50.0 \pm 7.6	1.5 \pm 0.2	0.03 \pm 0.01	1.4 \pm 0.2	3.6 \pm 0.6	2.3 \pm 0.4
CL3 18°C	42.8 \pm 4.7	2.7 \pm 0.4	0.08 \pm 0.01	1.4 \pm 0.2	3.5 \pm 0.5	1.9 \pm 0.2
Wild type 32°C	35.6 \pm 4.2	1.4 \pm 0.2	0.04 \pm 0.01	1.0 \pm 0.2	3.2 \pm 0.3	1.7 \pm 0.3
CL3 32°C	10.3 \pm 2.2	1.7 \pm 0.2	0.38 \pm 0.07	0.3 \pm 0.1	1.8 \pm 0.2	0.3 \pm 0.1

CL3 plants grown at 18°C had more developed and elongated chloroplasts (Fig. 2C) with both stacked and unstacked thylakoid membranes. Frequently, thylakoid membrane organization was altered in particular at the periphery of the chloroplast, and swollen stacked thylakoids were observed (Fig. 2D). In contrast, no significant differences in chloroplast ultrastructure were observed between wild-type plants grown at different temperatures (data not shown).

The severe effect on chloroplast ultrastructure observed in plants grown at standard light conditions of 100 $\mu\text{mol photons m}^{-2} \text{s}^{-1}$ prompted us to investigate ultrastructure of chloroplasts from plants grown under low-light conditions (10 $\mu\text{mol photons m}^{-2} \text{s}^{-1}$). Chloroplasts of both genotypes showed an essentially normal development of the internal membrane system with an increase in the fraction of the appressed thylakoid membranes as compared to those that had developed at 100 $\mu\text{mol photons m}^{-2} \text{s}^{-1}$ (Fig. 2, E–H). In CL3 plants, however, the chloroplasts were enlarged and displayed a somewhat rounded shape (Fig. 2E). Frequently, an enlarged thylakoid luminal space was discernible, mainly in stroma thylakoids and on the borders of grana stacks. Additionally, numerous vesicle-like structures appeared in these chloroplasts (Fig. 2, E and F).

Fluorescence Analyses

To assess whether Chl deficiency in the CL3 mutants was related to defects in pigment synthesis or loss in specific Chl-containing proteins, 77 K Chl fluorescence emission spectra of thylakoid suspensions from 6 d after germination seedlings were acquired (Fig. 3). Three major features are observed in the 77 K fluorescence emission spectra: A fluorescence band peaking at about 685 nm corresponds to emission from the PSII core antenna complex CP43 and light-harvesting complex II (LHCII). A further, usually less pronounced maximum at 695 nm is ascribed to the combined emissions of the PSII reaction center and the core antenna complex CP47. The most pronounced peak in the 77 K fluorescence emission spectra is observed at about 735 nm and originates from PSI emission. When normalized at 685 nm, a considerable decrease of the PSI peak relative to PSII was observed for the CL3 mutant, being more pronounced for 32°C-grown plants than for 18°C-

grown plants. Moreover, a pronounced 5-nm blue shift of the long wavelength PSI peak was observed.

The 77 K fluorescence data could indicate that primarily PSI is affected by the CL3 mutation. To further investigate this indication and to determine how PSI deficiency would affect overall photosynthetic efficiency and electron transport, room temperature Chl fluorescence was analyzed using a pulse amplitude modulation fluorometer.

The maximum photochemical efficiency of PSII in the dark-adapted state, F_v/F_m , was 0.812 and 0.755 for wild-type and CL3 mutant leaves, respectively, when the plants were grown at 18°C. When plants were grown at 32°C, F_v/F_m of wild-type plants was only slightly diminished (to 0.777) but the value for the CL3 mutant was drastically decreased to 0.361, indicating serious malfunction of PSII.

The response of the photochemical quenching parameter (qP) to increasing actinic light (AL) intensity for plants grown at different temperatures is shown in Figure 4A. Wild-type and the CL3 mutant plants responded in a dramatically different manner: Wild-type leaves grown at either temperature showed an almost identical—gradual—decrease of qP with increasing AL intensities. In contrast, the 18°C-grown CL3 plants displayed a dramatic decrease of qP already at moderate AL intensities, well below the growth light level, and CL3 plants grown at 32°C showed no photochemical quenching (i.e. photosynthetic activity) at all.

The light response of nonphotochemical quenching (quantified as NPQ) in wild-type and CL3 mutant plants grown at different temperatures is shown in Figure 4B. The largest capacity for NPQ buildup with increasing AL intensity was observed in 18°C-grown wild-type plants, whereas it was only slightly diminished in 32°C-grown wild-type plants and 18°C-grown CL3 plants. CL3 plants grown at 32°C, however, displayed a drastically diminished capacity to develop NPQ (Fig. 4B). Moreover, the observed NPQ in the latter plants corresponded almost entirely to the very slowly or nonrelaxing photoinhibitory quenching (data not shown).

Proteins of the Photosynthetic Apparatus

The fluorescence data indicate that both PSI and PSII are affected in the CL3 mutant, depending on the

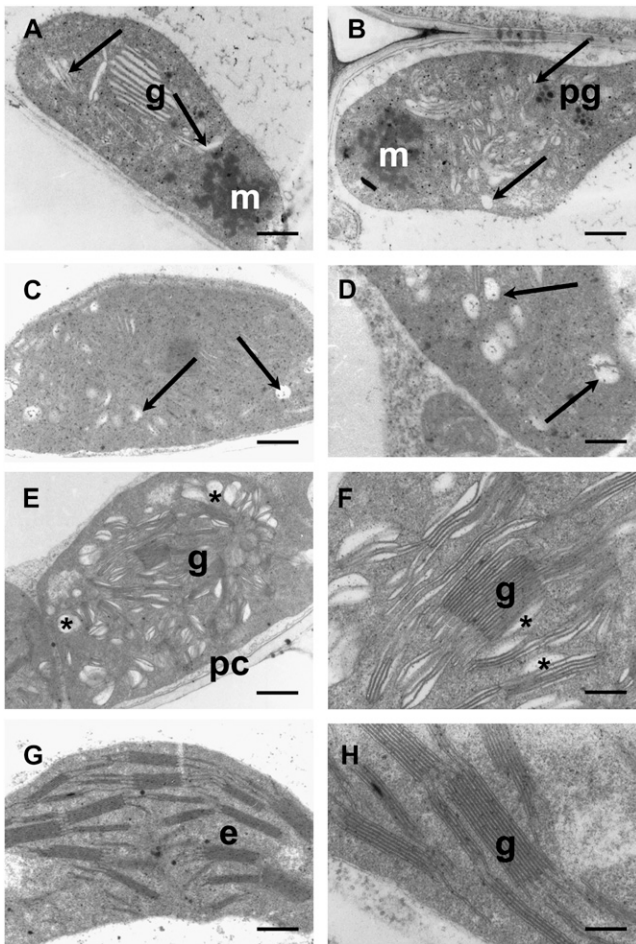


Figure 2. A and B, Chloroplast ultrastructure of 6 d after germination CL3 seedlings grown at $100 \mu\text{mol photons m}^{-2} \text{s}^{-1}$ fluorescent light, 32°C . C and D, Chloroplasts of CL3 seedlings grown at $100 \mu\text{mol photons m}^{-2} \text{s}^{-1}$ fluorescent light, 18°C . E and F, Chloroplast ultrastructure of 6 d after germination CL3 seedlings grown at $10 \mu\text{mol photons m}^{-2} \text{s}^{-1}$ incandescent light, 18°C . G and H, Chloroplasts of wild-type seedlings grown at $10 \mu\text{mol photons m}^{-2} \text{s}^{-1}$ incandescent light, 18°C . e, Stroma; g, grana; pc, cell wall; asterisks (*) and arrows indicate swollen thylakoids; m, electrodense material; pg, plastoglobuli. Scale bars: A, B, C, and G, $0.5 \mu\text{m}$; D, F, and H, $0.2 \mu\text{m}$; E, $0.8 \mu\text{m}$.

experimental conditions. To further investigate these responses, the amounts of different thylakoid proteins were determined by immunoblotting. Analyses of the D1 reaction center subunit of PSII and the major LHCII are presented in Figure 5. When the plants were grown at 18°C only little difference between wild-type and CL3 plants with respect to D1 and LHCII content was observed. In contrast, these proteins were considerably decreased in amount or even absent in the mutant when grown at 32°C . Absence of qP, considerably lowered F_v/F_m , and severe photoinhibition in these seedlings suggest that the disappearance of the D1 protein may result from a severely overreduced inter-system electron transport chain. To test this notion, the effects exerted by fluorescent light only were compared with those of a mixture of fluorescent and

incandescent light of the same light intensity ($100 \mu\text{mol photons m}^{-2} \text{s}^{-1}$; Fig. 5). Incandescent light is exciting PSI more efficiently (due to its higher proportion of far-red light) and therefore this light mixture should potentially reduce overreduction of the inter-system electron transport chain and excitation pressure on PSII. Indeed, under mixed light conditions, the D1 and LHCII proteins were observed in CL3 seedlings at approximately similar levels as in the wild type, even under growth at 32°C .

To circumvent the effects of severe photoinhibition we only used plants grown under mixed illumination for the analysis of PSI proteins (Supplemental Fig. S1). PsaC and PsaE were absent or almost undetectable in CL3 plants at both temperatures. However, PsaD was nearly undetectable in the mutant grown at 32°C , but when CL3 plants were grown at 18°C it appeared as a weak band after 3 d following germination and its level further increased at days 6 and 9. To more accurately quantify the amount of PSI subunits in the CL3 mutant, immunoblotting was carried out with different dilutions of thylakoids from the 6 d after germination seedlings grown at 18°C (Supplemental Fig. S2). This analysis shows that the amount of PsaA/B and PsaD in CL3 corresponded to approximately 10% to 25% of the wild-type levels. PsaE and PsaC could be detected, but the amounts were lower, particularly for PsaC that was present at less than 3% of the wild-type level. Immunoblots with antibodies against PsaF and LHCI subunits are shown in Supplemental Fig. S3. PsaF is essentially absent in CL3 at both temperatures, whereas little effect on LHCI proteins was seen. To determine whether the PSI deficiency is elicited at the transcriptional or posttranscriptional level, RNA was isolated and transcript levels for *psaC*, *psaD*, and *psaE* were determined by northern blotting. No significant differences in the transcript levels were found between the mutant and wild type, neither at 18°C nor at 32°C (data not shown).

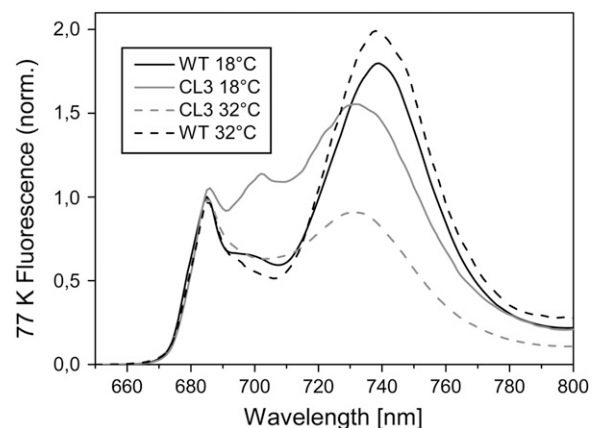


Figure 3. 77 K fluorescence spectra obtained with thylakoids from 6 d after germination seedlings grown at $100 \mu\text{mol photons m}^{-2} \text{s}^{-1}$ at 18°C and 32°C under a mixture of fluorescent and incandescent light. The spectra were normalized at 685 nm . WT, Wild type.

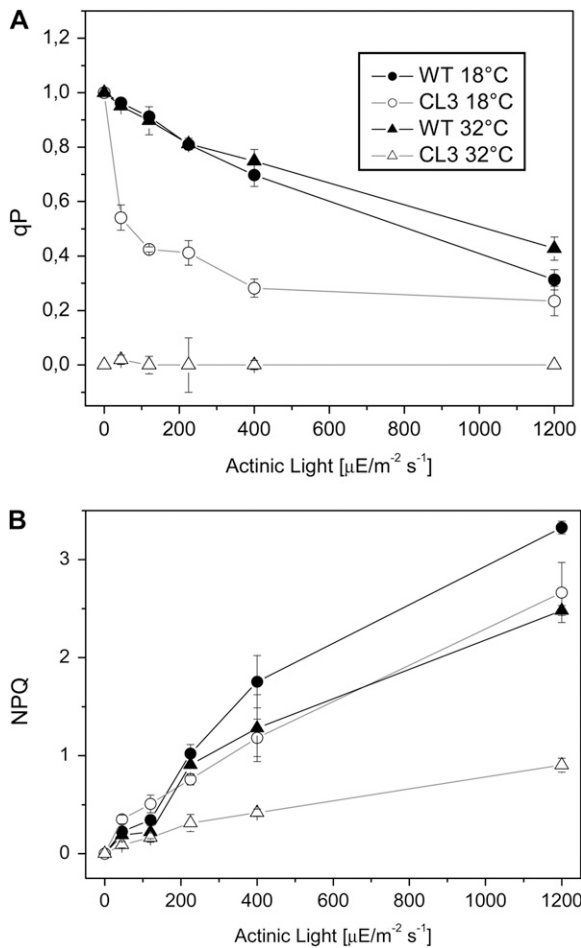


Figure 4. Photochemical quenching (A) and nonphotochemical quenching (B) of 6 d after germination seedlings grown at 100 $\mu\text{mol photons m}^{-2} \text{s}^{-1}$ at 18°C and 32°C under a mixture of fluorescent and incandescent light. WT, Wild type.

DNA Sequences of Putative Candidate Genes

The specific primary defect in PSI assembly and the secondary photoinhibitory effects on PSII suggested that either one of the plastid-encoded PSI subunits or a factor required for PSI assembly could be mutated. We therefore sequenced the plastid genes *psaA*, *psaB*, and *psaC* in the CL3 mutant and the sequences were identical to the published barley plastome (NC_008590).

The lack of direct effect on PSI genes prompted us to investigate the chloroplast genes *ycf3* or *ycf4*, which have been reported to be involved in PSI assembly (Boudreau et al., 1997; Naver et al., 2001; de Longevialle et al., 2008). The corresponding fragments of plastid DNA from CL3 mutant and wild type were amplified and sequenced. The sequence of *ycf4* was found to be identical in mutant and wild type, indicating that the CL3 phenotype was not related to *ycf4*. The complete *ycf3* sequence in barley consists of three exons (124, 230, and 159 bp long) split by two

introns (759 and 723 bp). The coding sequence of the *ycf3* gene recently published for barley (NC_008590) is identical to our wild-type sequence. However, two point mutations were found in intron 1 of the *ycf3* gene (Supplemental Fig. S4). These mutations are a T \rightarrow C substitution at nucleotide 528 and a T insertion between nucleotides 150 and 151.

ycf3 Transcripts

To assess the effects at the mRNA level of the mutations in intron 1 of *ycf3*, total RNA was isolated from wild type and mutant grown at 18°C and 32°C and analyzed by reverse transcription (RT)-PCR (Fig. 6). In the wild type, a band of about 500 bp, corresponding to the intronless fully spliced transcript (513 bp), was observed at both temperatures. However, two bands were observed in CL3 grown at 18°C, one of 513 bp corresponding to the intronless transcript, and another one between 1.2 and 1.5 kb, which, according to sequencing, corresponded to a larger processing intermediate of *ycf3* that contained the three exons plus additionally intron 1 (1.272 kb; Supplemental Fig. S5). Surprisingly, when seedlings were grown at 32°C, the band corresponding to the fully spliced transcript was absent in CL3 and the major band observed corresponded to the immature transcript of 1.272 kb. In silico fold analysis of the RNA sequence of intron 1 (Zuker and Stiegler, 1981) showed that the wild-type RNA is predicted to have a stable structure at both temperatures, whereas the CL3 RNA has a different structure and is predicted to change considerably between the two temperatures (Supplemental Fig. S6).

Analysis of the *ycf3* cDNA also revealed an editing site in exon 2 similar to one previously observed in maize (*Zea mays*; Ruf et al., 1994; Ruf and Kössel, 1997). It was also observed that editing in exon 2 had already occurred in the intron 1-containing transcript of *ycf3*

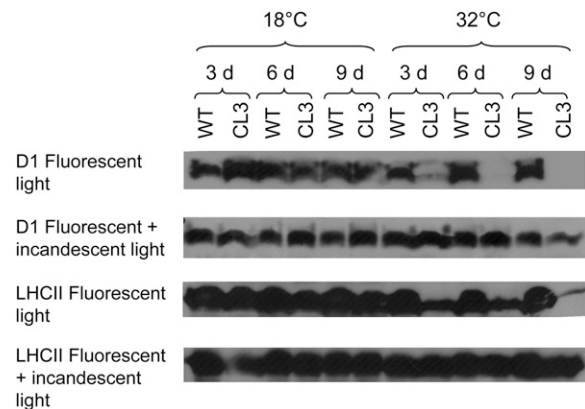


Figure 5. Immunoblot analyses of thylakoid protein extracts from wild-type (WT) and CL3 seedlings with antisera raised against D1 and LHCII. Equal amounts of Chl (1 μg) were loaded per lane. Thylakoid homogenates were extracted from seedlings of 3, 6, and 9 d after germination grown at 18°C or at 32°C under two different light environments at 100 $\mu\text{mol photons m}^{-2} \text{s}^{-1}$.

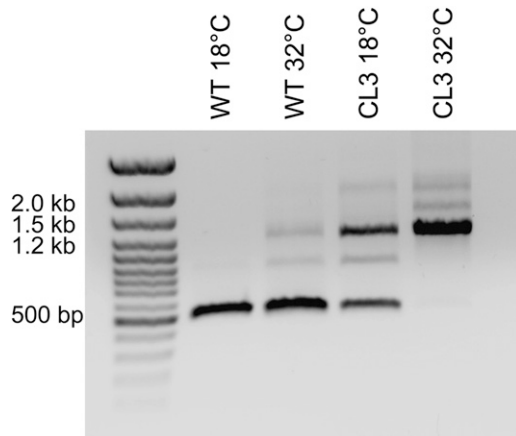


Figure 6. Analysis of *ycf3* transcripts by RT-PCR. RNA was isolated from 6 d after germination seedlings grown at $100 \mu\text{mol photons m}^{-2} \text{ s}^{-1}$ under a mixture of fluorescent and incandescent light. The size of the fragments in base pairs is indicated in lane 1. Lane 2, Wild type (WT) grown at 18°C ; lane 3, wild type grown at 32°C ; lane 4, CL3 grown at 18°C ; lane 5, CL3 grown at 32°C .

from CL3 as previously observed in intron 1-containing transcript of *ycf3* from maize (Ruf and Kössel, 1997; Supplemental Fig. S5). Interestingly, nucleotide 44 in exon 1, which is the other editing site in maize (Ruf et al., 1994; Ruf and Kössel, 1997), was already a T in barley.

To confirm that the inefficient splicing of *ycf3* transcript was a specific effect and not a general problem with mRNA processing, other transcriptional units containing introns were analyzed. Northern blots for *atpF* and *petB* transcripts showed no significant alterations in the transcript patterns of these two genes between CL3 mutant and wild type (data not shown).

Ycf3 Protein

To assess the amount of Ycf3 protein in wild type and CL3 we made an immunoblot with an antibody raised against a barley Ycf3 peptide (Fig. 7). Ycf3 was present in CL3 at 18°C but almost absent at 32°C . There appeared to be a higher amount of the chaperone in the mutant at 18°C compared to the wild type, however, this could be an effect of protein overloading as the gel was loaded on a Chl basis (Supplemental Fig. S7).

DISCUSSION

The mutant described here showed a dramatic phenotype at the restrictive temperature, and even at low light intensity the plants could not survive at 32°C beyond the seedling stage. The plants that had been grown under those conditions for 6 d after germination were pale green but not obviously affected in growth (Fig. 1B). At the permissive temperature of

18°C the CL3 mutant plants survive and they eventually set viable seed. Six days after germination the mutant plants did not show any visible symptoms except for a slight Chl deficiency (Fig. 1A). Closer inspection showed that even at the permissive conditions, the plants had an impaired PSI and severely decreased capacity for photosynthesis (Figs. 3 and 4). The amount of PSI in the thylakoids was severely decreased, especially at the higher temperature (Supplemental Figs. S1 and S2). Analysis of fluorescence also strongly indicated that PSI was primarily affected in the mutant. In general, PSI is known to be much more stable, also at high temperatures, than PSII (Berry and Björkman, 1980; Takeuchi and Thornber, 1994; Al-Khatib and Paulsen, 1999), but in the CL3 mutant PSI was more affected than PSII. The biochemical, spectroscopic, and physiological phenotype resembles that described for several other PSI mutants, where the amount of PSI is decreased and a secondary damage to PSII and other thylakoid proteins is observed especially at higher light intensity and with light that predominantly excites PSII (Haldrup et al., 2000, 2003).

PSI is a multisubunit pigment-protein complex embedded in the thylakoid membranes of chloroplasts and cyanobacteria. PSI catalyzes light-induced electron transfer from plastocyanin (and/or cytochrome *c* in certain cyanobacteria) to ferredoxin—ultimately leading to NADP reduction (for review, see Jensen et al., 2007). PSI is composed of at least 19 protein subunits in higher plants (Nelson and Yocum, 2006; Jensen et al., 2007). PsaA, PsaB, PsaC, PsaI, and PsaJ proteins are chloroplast encoded, while the other subunits are encoded by nuclear genes. PsaI and PsaJ are not essential for PSI function and assembly (Xu et al., 1995; Hansson et al., 2007), and we have therefore not investigated them in this study. PsaA and PsaB form the reaction center complex around which all other subunits are assembled. PsaC, PsaD, and PsaE are components of a stromal peripheral domain, which interacts with the intrinsic membrane proteins PsaH, PsaI, PsaL, and PsaO (Nelson and Yocum 2006; Jensen et al., 2007). The peripheral subunits are

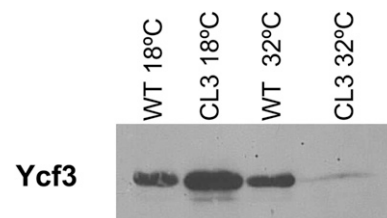


Figure 7. Immunoblot analysis of the amount of Ycf3 protein in thylakoid protein extracts. Thylakoid homogenates were extracted from seedlings 6 d after germination grown at 18°C or at 32°C under a mixture of fluorescent and incandescent light ($100 \mu\text{mol photons m}^{-2} \text{ s}^{-1}$). Equal amounts of Chl ($5 \mu\text{g}$) were loaded per lane. A corresponding Coomassie Brilliant Blue-stained gel is shown in Supplemental Figure S7. WT, Wild type.

essential for PSI function, whereas the H, I, L, and O subunits are not. It is generally assumed that the initial event in PSI assembly is the formation of a heterodimeric PsaA/PsaB core complex, followed by association of PsaC, which is required for subsequent binding of PsaD and PsaE (Choquet and Vallon, 2000; Chitnis, 2001; Fromme et al., 2001; Antonkine et al., 2003). In addition, PsaD was found to be essential for the stable binding of PsaC and PsaE (Li et al., 1991; Naver et al., 1995), and *Arabidopsis thaliana* mutants deficient in PsaD cannot assemble stable PSI (Haldrup et al., 2003; Ihnatowicz et al., 2007). While PsaC and PsaD seem to be essential for accumulation of stable PSI this is not the case for the other small subunits. Thus, although the PsaF subunit is essential for PSI function in plants, inactive PSI complexes lacking PsaF were present in *Arabidopsis* plants with down-regulated PsaF expression (Haldrup et al., 2000). Plants with decreased content of PsaF or PsaD had a low PSI activity and hence a strong tendency to overreduction of the intersystem chain, which made PSII highly susceptible to photodamage (Haldrup et al., 2000, 2003; Ihnatowicz et al., 2004). PSI with impaired function can also generate reactive oxygen, which may directly damage PSII (Tjus et al., 2001). In either case, the compromised photosynthesis will make it difficult for the plant to generate the energy required for PSII repair, thereby further exacerbating PSII photodamage. Other PSI mutants, e.g. when PsaE, PsaH, or PsaN are absent, still have a functional PSI, albeit with a decreased activity (Haldrup et al., 1999; Naver et al., 1999; Pesaresi et al., 2002; Ihnatowicz et al., 2007). In such cases the plants are able to respond with a change in PSI-to-PSII ratio and/or relative antenna size of the photosystems, and thereby limit redox imbalance and oxidative damage to either photosystem.

CL3 plants germinated under permissive conditions had some intact PSI complexes, but they accumulated very slowly and the PsaC, PsaE, and PsaF subunits were clearly substoichiometric compared to PsaA/B and PsaD (Supplemental Figs. S1–S3). This observation implies the presence of PSI complexes containing PsaA, PsaB, and PsaD but devoid of PsaC. This is a surprising finding. In the cyanobacterium *Anabaena* it has been found that inactivation of the *psaC* gene results in accumulation of PSI devoid of PsaC (Mannan et al., 1991). Whether the complexes contained PsaD was not reported. In contrast, *Chlamydomonas reinhardtii* with an inactivated *psaC* gene does not accumulate PSI, presumably because the entire complex becomes unstable in the absence of PsaC (Takahashi et al., 1991). The barley plants investigated in this study seem to have a response different from *C. reinhardtii* since PsaC appears not to be essential for accumulation of PSI, even though accumulation is inhibited substantially. Nevertheless, it should be born in mind, that PSI devoid of PsaC must be inactive, since PsaC carries the ultimate electron acceptors in PSI, iron sulfur clusters F_A and F_B, which are indispensable.

Given the specific effect of the CL3 mutation on PSI it seemed that the site of the mutation would be either in PSI itself or in a gene encoding a factor required for function of PSI. The PsaA, PsaB, and PsaC subunits are all required for PSI function, but in the CL3 mutant transcripts are present in normal amounts for all three proteins and they do not contain any differences from the wild-type transcripts. This caused us to look at two plastid genes that are known to encode factors specifically required for PSI assembly, i.e. *ycf3* and *ycf4* (Boudreau et al., 1997; Naver et al., 2001). While *ycf4* did not contain any differences in CL3 compared to wild type, we observed a dramatic difference with *ycf3*. In the CL3 plants the *ycf3* gene had two mutations in the noncoding intron 1 sequence and somehow this difference interfered with splicing of the first intron. Thus, the CL3 plants contain highly decreased amounts of the correct *ycf3* transcript at the permissive conditions and undetectable amounts at the restrictive conditions (Fig. 6). Sequences of *ycf3* homologs are conserved from cyanobacteria to higher plants: they consist of three exons and two group II introns in the latter (Maier et al., 1995). Group II introns have a ribozymic activity and adopt a conserved secondary structure (Michel and Ferat, 1995; Chu et al., 2001). In wild-type tobacco (*Nicotiana tabacum*), *ndhB* (a group II intron gene) pre-mRNA is blocked at high temperature (Karcher and Bock, 2002). One of the alternatives the authors proposed is that an aberrant RNA secondary structure formation of the intron at high temperature indirectly causes the splicing defect. In silico fold analysis of the RNA sequence of intron 1 from wild type and mutant showed that CL3 RNA is susceptible to change at different temperatures (Supplemental Fig. S6) and that temperature change in the mutant leads to disruption of the RNA secondary structure required for splicing the intron, especially at 32°C.

Interestingly, an *Arabidopsis* mutant deficient in splicing of intron 2 of *ycf3* has been described (de Longevialle et al., 2008). The primary defect is in a nuclear gene *OTP51* that is specifically required for splicing of this particular intron. The *otp51* mutant does not contain detectable Ycf3 and PSI.

In spite of the decreased amount of *ycf3* transcript at the permissive temperature, the amount of Ycf3 protein was not affected (Fig. 7). However, at the higher temperature the protein was almost missing in CL3. This result explains the presence of a functional PSI at 18°C in the mutant and the incomplete assembly of PSI at the restrictive temperature.

In *ycf3*-deficient *C. reinhardtii* the PSI proteins PsaA, PsaD, PsaC, and PsaF were undetectable (Boudreau et al., 1997). Surprisingly, the Ycf3-deficient thylakoids still contained detectable PsaE, but this protein must have been associated with non-PSI proteins in the membranes (Boudreau et al., 1997). In contrast, in CL3 mutant, PsaA could be observed while PsaE was highly reduced. A tobacco mutant with a completely deleted *ycf3* gene displayed a light-sensitive

phenotype, lacked PSI, and was photosynthetically inactive (Ruf et al., 1997).

For *C. reinhardtii* it has been demonstrated that the Ycf3 protein is required for PSI assembly, acting as a chaperone that interacts with the PSI subunits PsaA and PsaD (Naver et al., 2001). These authors also generated a temperature-sensitive mutant with an altered Ycf3 protein, which did not accumulate PSI when grown above a restrictive temperature. The conditional Ycf3 mutant allowed Naver et al. (2001) to generate intact PSI in *C. reinhardtii* lacking Ycf3, and they could exclude that Ycf3 plays any role in PSI stability. As discussed above, PSI in plants can assemble in the absence of most small subunits, and only PsaC and PsaD are absolutely required for accumulation of PSI complexes. Hence, Ycf3 would likely be involved in integrating one or both of these subunits in the PSI complex, and this agrees with the observed interaction of Ycf3 with PsaA and PsaD (Naver et al., 2001). It should be pointed out that the studies of Naver et al. (2001) did not exclude that Ycf3 may interact with PsaC as well.

CONCLUSION

Despite several studies it is still not clear how the Ycf3 protein assists the assembly of PSI. The tobacco and *C. reinhardtii* mutants lacking Ycf3 do not assemble PSI, but in this study, some PSI assembly took place, especially of PsaD, whereas PsaC assembly appeared to be almost completely inhibited. Given the total absence of PSI in *ycf3* null mutants, the PSI present in the CL3 mutant is due to the presence of Ycf3 protein. Immunoprecipitation has shown that Ycf3 interacts with PsaD, although it could not be excluded that Ycf3 also interacts with other PSI subunits (Naver et al., 2001). This study indicates that Ycf3 has a specific role in assembly of PsaC with the PSI complex.

MATERIALS AND METHODS

Plant Material and Growth Conditions

Seedlings of two-row spring barley (*Hordeum vulgare* CL3; Prina 1996) and MC182 (accession no. of the Institute for Genetics, Instituto Nacional de Tecnología Agropecuaria) as wild-type control were grown at 18°C or 32°C with a 16-h photoperiod. Two models of growth chambers were used: a Sanyo-type (with fluorescent tubes only) and a Conviron-type chamber (with fluorescent tubes and incandescent lamps) and in both cases the light intensity was 100 $\mu\text{mol photons m}^{-2} \text{s}^{-1}$. In one of the experiments, seedlings were cultivated under low-light conditions (incandescent light of 10 $\mu\text{mol photons m}^{-2} \text{s}^{-1}$). All the experiments were carried out on primary leaves and unless otherwise noted the leaves were from 6 d after germination seedlings grown in the Conviron chamber with a mix of incandescent and fluorescent light at 100 $\mu\text{mol photons m}^{-2} \text{s}^{-1}$.

Pigment Analyses

Pigment analyses were performed as described previously (Lokstein et al., 2002): Leaf tissue was frozen in liquid nitrogen and stored at -80°C until extraction. Pigments were analyzed by HPLC on a Waters chromatography

system (600 E gradient module, 717 autosampler, 996 diode array detector) using a Waters Spherisorb ODS2 analytical column (5 μm particle size; $4.6 \times 250 \text{ mm}$). Gradients consisted of acetonitrile:water:triethylamine (900:100:1, solvent A) and ethyl acetate (solvent B) with 100% A for 16 min, 66.7% A/33.3% B for 6 min, 59.7% A/40.3% B for 12 min, 33.3% A/66.7% B for 0.2 min, 100% B for 2.5 min, and 100% A for 4.3 min. The flow rate was 1 mL min^{-1} . Pigments were identified by their specific retention times and absorption spectra and quantified by comparison to authentic standards using photodiode array detection at 440 nm.

Transmission Electron Microscopy

Small samples (about 2 mm thick) of first-leaf blades were fixed overnight in 2.5% glutaraldehyde in 0.1 M phosphate buffer, pH 7.2, at 4°C, postfixed in 1% osmium tetroxide in water for 2 h at 4°C, dehydrated in a graded ethanol-acetone series, and embedded in Spurr's resin. Semithin sections (1 μm thick) and ultrathin sections for light and transmission electron microscopy, respectively, were obtained with an ultramicrotome (Reichert-Jung). Semithin sections were stained with 1% toluidine blue O (Sigma) and examined in an Axioskop 2 Zeiss photomicroscope. Ultrathin sections were mounted on grids, stained with lead citrate followed by uranyl acetate, and examined in a Zeiss EM109T transmission electron microscope.

Fluorescence Analyses

In vivo Chl fluorescence was measured using a pulse amplitude modulation fluorometer (FMS 2, Hansatech) with attached leaves as previously described (Lokstein et al., 2002). Fluorescence parameters were calculated as follows: $F_v/F_m = (F_m - F_0)/F_m$ is the maximum photochemical efficiency of PSII, in the dark-adapted state. Nonphotochemical quenching was quantified as NPQ = $(F_m/F_m') - 1$. Photochemical quenching was quantified as qP = $(F_m' - F_m)/(F_m' - F_0')$. Photon flux densities were measured and adjusted using a quantum sensor (LI-COR, LI-189A).

77 K fluorescence emission spectra were recorded using a Fluorolog FL-112 spectrofluorometer with a 1680 emission double monochromator (Jobin-Yvon). Thylakoid membranes were suspended in 66% (v/v) glycerol/20 mM Tricine, pH 7.8, to a final Chl concentration of 2.5 $\mu\text{g mL}^{-1}$ and immediately dropped into liquid nitrogen. Frozen pearls were transferred to a Dewar vessel mounted in the fluorometer. Excitation was at 440 nm.

DNA Isolation, PCR, and Sequencing

Total DNA was extracted from leaves following a standard protocol (Fang et al., 1992). PCRs for sequencing *ycf3* gene were performed using 20 ng of DNA, 2 \times Taq buffer, 1 mM MgSO_4 , 0.32 μM of each primer, 0.32 mM dNTP mix, and 2.5 units Platinum Taq Pfx (Invitrogen). Following denaturation at 94°C for 5 min, the reaction mixtures were heated to 94°C for 15 s, 55°C for 30 s, and 68°C for 1 min, in 30 cycles. PCR fragments were cloned into pCR4 Blunt-TOPO (Zero Blunt TOPO PCR cloning kit for sequencing, Invitrogen). Three independent colonies of each genotype were sequenced. Sequence data alignments (Chenna et al., 2003) were performed using the ClustalW WWW service at the European Bioinformatics Institute (<http://www.ebi.ac.uk/blast/>). PCRs for amplifying the cDNA were performed using 20 ng of DNA, 1 \times Taq buffer, 3 mM MgCl_2 , 0.25 μM of each primer, 0.25 mM of deoxynucleotide triphosphate mix, and 1 unit Taq DNA polymerase (Invitrogen).

The sequence of *ycf3* gene was amplified by PCR with primers designed on the basis of published information of the chloroplast DNA sequence of wheat (*Triticum aestivum*; GenBank NC_002762). A fragment of 2 kb was amplified using primer P1, 5'-TTATTCAAATTCAAAGCGCTTCGTA-3' and primer P6, 5'-ATGCCATAGATCCCGTGTAATGGAA-3'. Four internal primers were designed for sequencing, P0, 5'-CTAAGTTTCAAACCCTAATTTTAT-3'; P2, 5'-TTTTTTAGTGTATCGACCCAGTCGC-3'; P3, 5'-GCCCGGAAA-TAATATTCCAAAGCCT-3'; P4, 5'-CACCAATGAATCTATTAATGCTA-3'.

RNA Isolation and Analysis

Total RNA was isolated from leaves with Trizol (Invitrogen). RNA for RT was digested with DNase RQ1 (Promega). cDNA was synthesized with SuperScript III reverse transcriptase using the antisense primer P1, according to the manufacturer's instructions (Invitrogen). Products of RT were amplified

by PCR as described above and cloned into pCR2.1-TOPO vector (TOPO TA cloning kit, Invitrogen). Three independent colonies of each genotype were sequenced.

Thylakoid Membrane Isolation and Immunoblotting

Thylakoid membranes were isolated according to Guimét et al. (2002). Thylakoid proteins were separated by SDS-PAGE and immunoblotted with several antibodies to determine the presence or absence of different polypeptides. Solubilized thylakoids of each sample corresponding to the same amount of Chl were electrophoresed in 13% (w/v) SDS-polyacrylamide gels. Separated proteins were transferred to nitrocellulose membranes and probed with rabbit antibodies raised against PSI core complex (recognizing PsaA/B, C, D, E, L), PsaF, Lhca1, Lhca3, Lhca4, Lhcb1, and Lhcb2, LHCI (kindly provided by J.J. Guimét, INFIVE, Universidad de La Plata, Argentina) and D1 (kindly provided by Prof. A. Barkan, University of Oregon). The immunodetection procedures were performed with the ECL western-blotting analysis system (Amersham) according to the manufacturer's description and using horseradish peroxidase-conjugated donkey-anti-rabbit secondary antibody. The polyclonal antibody against barley Ycf3 was produced in rabbits immunized with a synthetic peptide with the sequence EAMRLEIDPYDRSYC coupled to keyhole limpet hemocyanin (GenScript Corp.). Immunodetection of Ycf3 was accomplished with the SuperSignal West Dura extended duration substrate (Pierce) according to the manufacturer's description and using horseradish peroxidase-conjugated goat-anti-rabbit secondary antibody.

Supplemental Data

The following materials are available in the online version of this article.

Supplemental Figure S1. Immunoblot analysis of thylakoid protein extracts from wild-type and CL3 seedlings with antisera raised against PSI.

Supplemental Figure S2. Immunoblot analysis of dilutions of thylakoid protein extracts from wild-type and CL3 seedlings with antisera raised against PSI.

Supplemental Figure S3. Immunoblot analyses of thylakoid protein extracts from wild-type and CL3 seedlings with antisera raised against the polypeptides indicated on the left side.

Supplemental Figure S4. DNA sequence alignment of *ycf3* gene from wild type, CL3, and wheat.

Supplemental Figure S5. Sequence alignment of *ycf3* gene DNA from wild-type and CL3 intron 1-containing *ycf3* cDNA.

Supplemental Figure S6. RNA fold prediction of *ycf3* intron 1: A, wild type, 18°C; B, CL3, 18°C; C, wild type, 32°C; D, CL3, 32°C.

Supplemental Figure S7. SDS-PAGE gel stained with Coomassie Brilliant Blue corresponding to immunoblot against Ycf3 protein (Fig. 7).

ACKNOWLEDGMENTS

Drs. A. Barkan and J.J. Guimét are thanked for providing antibodies against LHCI and D1. We also would like to thank Prof. Thomas Börner for support, Dr. Fernando Ardila and Dr. Craig Simpson for technical advice, and Mr. Abel Mario Moglie for his skillful technical assistance in handling and maintaining the experimental plant material.

Received September 21, 2009; accepted October 5, 2009; published October 7, 2009.

LITERATURE CITED

Al-Khatib K, Paulsen GM (1999) High-temperature effects on photosynthetic processes in temperate and tropical cereals. *Crop Sci* **39**: 119–125
Antonkine ML, Jordan P, Fromme P, Krauss N, Golbeck JH, Stehlik D (2003) Assembly of protein subunits within the stromal ridge of photosystem I: structural changes between unbound and sequentially PSI-

bound polypeptides and correlated changes of the magnetic properties of the terminal iron sulfur clusters. *J Mol Biol* **327**: 671–697

Berry J, Björkman O (1980) Photosynthetic response and adaptation to temperature in higher plants. *Annu Rev Plant Physiol* **31**: 491–543

Boudreau E, Takahashi Y, Lemieux C, Turmel M, Rochaix JD (1997) The chloroplast *ycf3* and *ycf4* open reading frames of *Chlamydomonas reinhardtii* are required for the accumulation of the photosystem I complex. *EMBO J* **16**: 6095–6104

Chenna R, Sugawara H, Koike T, Lopez R, Gibson TJ, Higgins DG, Thompson JD (2003) Multiple sequence alignment with the Clustal series of programs. *Nucleic Acids Res* **31**: 3497–500

Chitnis PR (2001) Photosystem I: function and physiology. *Annu Rev Plant Physiol Plant Mol Biol* **52**: 593–626

Choquet Y, Vallon O (2000) Synthesis, assembly and degradation of thylakoid membrane proteins. *Biochimie* **82**: 615–634

Chu VT, Adamidi C, Liu Q, Perlman PS, Pyle AM (2001) Control of branch-site choice by a group II intron. *EMBO J* **20**: 6866–6876

de Longevialle AF, Hendrickson L, Taylor NL, Delannoy E, Lurin C, Badger M, Millar AH, Small I (2008) The pentatricopeptide repeat gene OTP51 with two LAGLIDADG motifs is required for the cis-splicing of plastid *ycf3* intron 2 in *Arabidopsis thaliana*. *Plant J* **56**: 157–168

Fang G, Hammar S, Grumet R (1992) A quick and inexpensive method for removing polysaccharides from plant genomic DNA. *Biotechniques* **56**: 52–54

Fromme P, Jordan P, Krauss N (2001) Structure of photosystem I. *Biochim Biophys Acta* **1507**: 5–31

Guimét JJ, Tyystjärvi E, Tyystjärvi T, John I, Kairavuo M, Pichersky P, Noodén LD (2002) Photoinhibition and loss of photosystem II reaction center proteins during senescence of soybean leaves: enhancement of photoinhibition by the “stay-green” mutation *cytG*. *Physiol Plant* **115**: 468–478

Gustafsson A (1942) The plastid development in various types of chlorophyll mutations. *Hereditas* **28**: 483–492

Haldrup A, Lunde C, Scheller HV (2003) *Arabidopsis thaliana* plants lacking the PSI-D subunit of photosystem I suffer severe photoinhibition, have unstable photosystem I complexes, and altered redox homeostasis in the chloroplast stroma. *J Biol Chem* **278**: 33276–33283

Haldrup A, Naver H, Scheller HV (1999) The interaction between plastocyanin and photosystem I is inefficient in transgenic *Arabidopsis* plants lacking the PSI-N subunit of photosystem I. *Plant J* **17**: 689–698

Haldrup A, Simpson DJ, Scheller HV (2000) Down-regulation of the PSI-F subunit of photosystem I (PSI) in *Arabidopsis thaliana*. *J Biol Chem* **275**: 31211–31218

Hansson A, Amann K, Zygadlo A, Meurer J, Scheller HV, Jensen PE (2007) Knock-out of the chloroplast-encoded PSI-J subunit of photosystem I in *Nicotiana tabacum*: PSI-J is required for efficient electron transfer and stable accumulation of photosystem I. *FEBS J* **274**: 1734–1746

Hess WR, Börner T (1999) Organellar RNA polymerases of higher plants. *Int Rev Cytol* **190**: 1–59

Ihnatowicz A, Pesaresi P, Leister D (2007) The E subunit of photosystem I is not essential for linear electron flow and photoautotrophic growth in *Arabidopsis thaliana*. *Planta* **226**: 889–895

Ihnatowicz A, Pesaresi P, Varotto C, Richly E, Schneider A, Jahns P, Salamini F, Leister D (2004) Mutants for photosystem I subunit D of *Arabidopsis thaliana*: effects on photosynthesis, photosystem I stability and expression of nuclear genes for chloroplast functions. *Plant J* **37**: 839–852

Jensen PE, Bassi R, Boekema EJ, Dekker JP, Jansson S, Leister D, Robinson C, Scheller HV (2007) Structure, function and regulation of plant photosystem I. *Biochim Biophys Acta* **1767**: 335–352

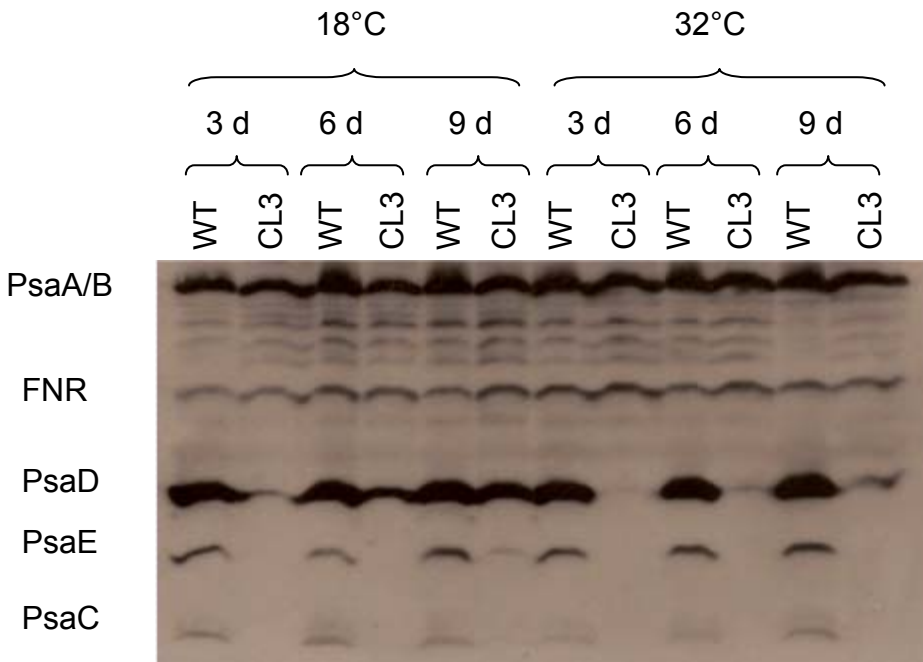
Karcher D, Bock R (2002) Temperature sensitivity of RNA editing and intron splicing reactions in the plastid *ndhB* transcript. *Curr Genet* **41**: 48–52

Leon P, Arroyo A, Mackenzie S (1998) Nuclear control of plastid and mitochondrial development in higher plants. *Annu Rev Plant Physiol Plant Mol Biol* **49**: 453–480

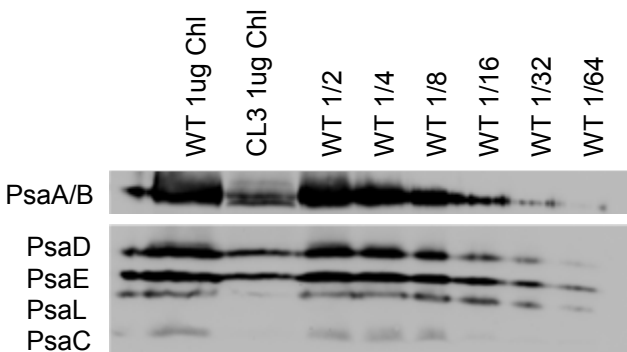
Li N, Zhao J, Warren PV, Warden JT, Bryant DA, Golbeck JH (1991) PsaD is required for the stable binding of PsaC to the photosystem I core protein of *Synechococcus* sp. PCC 6301. *Biochemistry* **30**: 7863–7872

Lokstein H, Tian L, Polle J, DellaPenna D (2002) Xanthophyll biosynthetic mutants of *Arabidopsis thaliana*: altered nonphotochemical quenching of chlorophyll fluorescence is due to changes in photosystem II antenna size and stability. *Biochim Biophys Acta* **1553**: 309–319

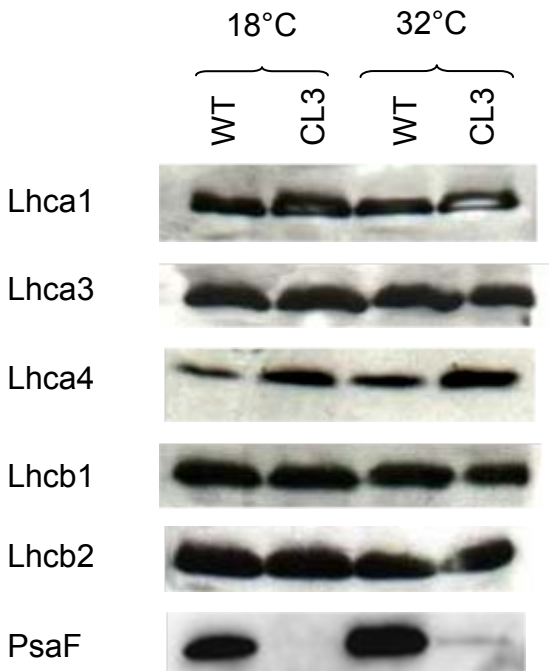
- Maier RM, Neckermann K, Igloi GL, Kössel H** (1995) Complete sequence of the maize chloroplast genome: gene content, hotspots of divergence and fine tuning of genetic information by transcript editing. *J Mol Biol* **251**: 614–628
- Mannan RM, Whitmarsh J, Nyman P, Pakrasi HB** (1991) Directed mutagenesis of an iron-sulfur protein of the photosystem I complex in the filamentous cyanobacterium *Anabaena variabilis* ATCC 29413. *Proc Natl Acad Sci USA* **88**: 10168–10172
- Michel F, Ferat JL** (1995) Structure and activities of group II introns. *Annu Rev Biochem* **64**: 435–461
- Naver H, Boudreau E, Rochaix JD** (2001) Functional studies of *Ycf3*: its role in assembly of photosystem I and interactions with some of its subunits. *Plant Cell* **13**: 2731–2745
- Naver H, Haldrup A, Scheller HV** (1999) Cosuppression of photosystem I subunit PSI-H in *Arabidopsis thaliana*: efficient electron transport and stability of photosystem I is dependent upon the PSI-H subunit. *J Biol Chem* **274**: 10784–10789
- Naver H, Scott MP, Andersen B, Möller BL, Scheller HV** (1995) Reconstitution of barley photosystem I reveals that the N-terminus of the PSI-D subunit is essential for tight binding of PSI-C. *Physiol Plant* **95**: 19–26
- Nelson N, Yocum CF** (2006) Structure and function of photosystems I and II. *Annu Rev Plant Biol* **57**: 521–565
- Pesaresi P, Lunde C, Jahns P, Tarantino D, Meurer J, Varotto C, Hirtz RD, Soave C, Scheller HV, Salamini F, et al** (2002) A stable LHCII-PSI aggregate and suppression of photosynthetic state transitions in the *psae1-1* mutant of *Arabidopsis thaliana*. *Planta* **215**: 940–948
- Prina AR** (1992) A mutator nuclear gene inducing a wide spectrum of cytoplasmically inherited chlorophyll deficiencies in barley. *Theor Appl Genet* **85**: 245–251
- Prina AR** (1996) Mutator induced cytoplasmic mutants in barley: genetic evidence of activation of a putative chloroplast transposon. *J Hered* **87**: 385–389
- Prina AR, Maldonado S, Arias MC, Colombo N, Rios RD, Acevedo A, Otegui M** (1996) Mutator induced variability in barley. *In* A Slinkard, G Scoles, B Rossnagel, eds, *Barley Genetics VII*, Ed 2, Vol 2. University of Saskatchewan, Saskatoon, Canada, pp 552–554
- Ruf S, Kössel H** (1997) Tissue-specific and differential editing of the two *ycf3* editing sites in maize plastids. *Curr Genet* **32**: 19–23
- Ruf S, Kössel H, Bock R** (1997) Targeted inactivation of a tobacco intron-containing open reading frame reveals a novel chloroplast-encoded photosystem I-related gene. *J Cell Biol* **139**: 95–102
- Ruf S, Zeltz P, Kössel H** (1994) Complete RNA editing of unspliced and dicistronic transcripts of the intron-containing reading frame IRF170 from maize chloroplasts. *Proc Natl Acad Sci USA* **91**: 2295–2299
- Smillie RM, Henningsen KW, Bain JM, Critchley C, Fester T, von Wettstein D** (1978) Mutants of barley heat-sensitive for chloroplast development. *Carlsberg Res Commun* **43**: 351–364
- Takahashi Y, Goldschmidt-Clermont M, Soen SY, Franzén LG, Rochaix JD** (1991) Directed chloroplast transformation in *Chlamydomonas reinhardtii*: insertional inactivation of the *psaC* gene encoding the iron sulfur protein destabilizes photosystem I. *EMBO J* **10**: 2033–2040
- Takeuchi TS, Thornber JP** (1994) Heat-induced alterations in thylakoid membrane protein composition in barley. *Aust J Plant Physiol* **21**: 759–770
- Taylor WC, Barkan A, Martienssen RA** (1987) Use of nuclear mutants in the analysis of chloroplast development. *Dev Genet* **8**: 305–320
- Tjus SE, Scheller HV, Andersson B, Möller BL** (2001) Active oxygen produced during selective excitation of photosystem I is damaging not only to photosystem I but also to photosystem II. *Plant Physiol* **125**: 2007–2015
- Von Wettstein D** (1961) Nuclear and cytoplasmic factors in development of chloroplast structure and function. *Can J Bot* **39**: 1537–1545
- Von Wettstein D, Gough S, Kannangara CG** (1995) Chlorophyll biosynthesis. *Plant Cell* **7**: 1039–1067
- Xu Q, Hoppe D, Chitnis VP, Odom WR, Guikema JA, Chitnis PR** (1995) Mutational analysis of photosystem I polypeptides in the cyanobacterium *Synechocystis* sp. PCC 6803. *J Biol Chem* **270**: 16243–16250
- Zuker M, Stiegler P** (1981) Optimal computer folding of large RNA sequences using thermodynamics and auxiliary information. *Nucleic Acids Res* **9**: 133–148



S. Figure S1. Immunoblot analysis of thylakoid protein extracts from WT and CL3 seedlings with antisera raised against PSI. Equal amounts of chlorophyll (1 μg) were loaded per lane. Thylakoid homogenates were extracted from seedlings of 3, 6 and 9 days after germination grown at 18°C or at 32°C under a mixture of fluorescent and incandescent light (100 $\mu\text{mol photons m}^{-2} \text{s}^{-1}$). FNR: ferredoxin:NADP⁺ reductase.



S. Figure S2. Immunoblot analysis of dilutions of thylakoid protein extracts from WT and CL3 seedlings with antisera raised against PSI. Lanes 1 and 2 were loaded with 1 μg chlorophyll of WT and CL3 thylakoid proteins, and lanes 3 to 8 were loaded with dilutions of the WT thylakoid extracts as indicated. Thylakoids were extracted from 6 days after germination seedlings grown at 18°C under a mixture of fluorescent and incandescent light (100 $\mu\text{mol photons m}^{-2} \text{s}^{-1}$).



S. Figure S3. Immunoblot analyses of thylakoid protein extracts from WT and CL3 seedlings with antisera raised against the polypeptides indicated on the left side. Equal amounts of chlorophyll (1 μg) were loaded per lane. Thylakoid homogenates were extracted from seedlings 6 days after germination grown at 18°C or at 32°C under a mixture of fluorescent and incandescent light (100 $\mu\text{mol photons m}^{-2} \text{s}^{-1}$).

WT	ycf3	ATGCCTAGATCCCCTGTAATGGAATTTTCATTGATAAGACCTTCTCAATTATAGCCAAT	60
CL3	ycf3	ATGCCTAGATCCCCTGTAATGGAATTTTCATTGATAAGACCTTCTCAATTATAGCCAAT	60
wheat	ycf3	ATGCCTAGATCCCCTGTAATGGAATTTTCATTGATAAGACCTTCTCAATTATAGCCAAT *****	60
WT	ycf3	ATTTTATTGCGAATAAATCCGACAACCTCAGGAGAAAAAAGGCATTTACTTTATATAGA	120
CL3	ycf3	ATTTTATTGCGAATAAATCCGACAACCTCAGGAGAAAAAAGGCATTTACTTTATATAGA	120
wheat	ycf3	ATTTTATTGCGAATAAATCCGACAACCTCAGGAGAAAAAAGGCATTTACTTTATATAGA *****	120
WT	ycf3	GATGTTGCGATTTGACTCTTTTTTTTTT	179
CL3	ycf3	GATGTTGCGATTTGACTCTTTTTTTTTT	180
wheat	ycf3	GATGTTGCGATTTGACTCTTTTTTTTTT---GCTTTTTTTAGCCCTACCTATACCTCAGT *****	176
WT	ycf3	CTTAGGAAAAGAAAAGGGTTGGCATAGAGAGAACCAAAATTTGTAAGCAAGCAAAACCC	239
CL3	ycf3	CTTAGGAAAAGAAAAGGGTTGGCATAGAGAGAACCAAAATTTGTAAGCAAGCAAAACCC	240
wheat	ycf3	CTTAGGAAAAGAAAAGGGTTGGCATAGAGAGAACCAAAATTTGTAAGCAAGCAAAACCC ****	236
WT	ycf3	ACGCTTCGGGAAGGTGAGGCGAACTAACAATTCCTCCGTCTGTATCCTCGATTGATGC	299
CL3	ycf3	ACGCTTCGGGAAGGTGAGGCGAACTAACAATTCCTCCGTCTGTATCCTCGATTGATGC	300
wheat	ycf3	ACGCTTCGGGAAGGTGAGGCGAACTAACAATTCCTCCGTCTGTATCCTCGATTGATGC *****	296
WT	ycf3	GGCTTCAGATACTTCAATTGTAGATTTGAGTATTGAGCGAAAAGTTACACCTACAGGATA	359
CL3	ycf3	GGCTTCAGATACTTCAATTGTAGATTTGAGTATTGAGCGAAAAGTTACACCTACAGGATA	360
wheat	ycf3	GGCTTCAGATACTTCAATTGTAGATTTGAGTATTGAGCGAAAAGTTACACCTACAGGATA *****	356
WT	ycf3	TGGTATGGTATGGATTACAGGCCA-----CTCTATTAGTATCCGTAGGCAGCATAGGGG	413
CL3	ycf3	TGGTATGGTATGGATTACAGGCCA-----CTCTATTAGTATCCGTAGGCAGCATAGGGG	414
wheat	ycf3	TGGTATGGTATGGATTACAGGCCAATCCTACTCTATTAGTATCCGTAGGCAGCATAGGGG *****	416
WT	ycf3	AGAAAAGCACTACACCTAGAAATAGGAATCAACAAGAGAAAACTTTGGTAGAAATTACC	473
CL3	ycf3	AGAAAAGCACTACACCTAGAAATAGGAATCAACAAGAGAAAACTTTGGTAGAAATTACC	474
wheat	ycf3	AGAAAAGCACTACACCTAGAAATAGGAATCAACAAGAGAAAACTTTGGTAGAAATTACC *****	476
WT	ycf3	CCTTTCCTGATCGGTATCAGGGCTGGGAAGAATGGTTGGGATAACAACAACCA	533
CL3	ycf3	CCTTTCCTGATCGGTATCAGGGCTGGGAAGAATGGTTGGGATAACAACAACCA	534
wheat	ycf3	CCTTTCCTGATCGGTATCAGGGCTGGGAAGAATGGTTGGGATAACAACAACCA *****	536
WT	ycf3	TTGTACTTTGGATACCCCTATAACCATCAAAGATCGTTGAAGTAGCTAATTCCTCTAAAT	593
CL3	ycf3	TTGTACTTTGGATACCCCTATAACCATCAAAGATCGTTGAAGTAGCTAATTCCTCTAAAT	594
wheat	ycf3	TTGTACTTTGGATACCCCTATAACCATCAAAGATCGTTGAAGTAGCTAATTCCTCTAAAT *****	596
WT	ycf3	AGGAGGCGTTGAGAACAAAGAAATTTGGAGCTATCGTTTTCTCTAGCATTAAATAGAA	653
CL3	ycf3	AGGAGGCGTTGAGAACAAAGAAATTTGGAGCTATCGTTTTCTCTAGCATTAAATAGAA	654
wheat	ycf3	AGGAGGCGTTGAGAACAAAGAAATTTGGAGCTATCGTTTTCTCTAGCATTAAATAGAA *****	656
WT	ycf3	TTTATTGGTGTAAAGAAAACTCTTGTGGGAAGGTTGGCTAGAGATTTCTGGAAAAAT	713
CL3	ycf3	TTTATTGGTGTAAAGAAAACTCTTGTGGGAAGGTTGGCTAGAGATTTCTGGAAAAAT	714
wheat	ycf3	TTTATTGGTGTAAAGAAAACTCTTGTGGGAAGGTTGGCTAGAGATTTCTGGAAAAAT *****	716
WT	ycf3	ACCAGCCCCTTTGCGTTTATAATGAGACGGGACTAATTCATTTTATTGATTCTATAGATTAA	773
CL3	ycf3	ACCAGCCCCTTTGCGTTTATAATGAGACGGGACTAATTCATTTTATTGATTCTATAGATTAA	774
wheat	ycf3	ACCAGCCCCTTTGCGTTTATAATGAGACGGGACTAATTCATTTTATTGATTCTATAGATTAA *****	775
WT	ycf3	GATTATTTGCGTTAGTACTATTATGTACAGAAGGGAGGAGCCGTATGAGATGAAAACCTC	833
CL3	ycf3	GATTATTTGCGTTAGTACTATTATGTACAGAAGGGAGGAGCCGTATGAGATGAAAACCTC	834
wheat	ycf3	-----TTTCGCTTAGTACTATTATGTACAGAAGGGAGGAGCCGTATGAGATGAAAACCTC *****	830
WT	ycf3	ATGTACGGTTTTGGAACGGAGATTTTTGAATAGAATGAACGACCGTAACGGATGTTGGC	893
CL3	ycf3	ATGTACGGTTTTGGAACGGAGATTTTTGAATAGAATGAACGACCGTAACGGATGTTGGC	894
wheat	ycf3	ATGTACGGTTTTGGAACGGAGATTTTTGAATAGAATGAACGACCGTAACGGATGTTGGC *****	890
WT	ycf3	TCAATCCGAAGGAAATATGCGGAAGCTTTGCAAAATTTATTGAAGCTACGCGACTAGA	953
CL3	ycf3	TCAATCCGAAGGAAATATGCGGAAGCTTTGCAAAATTTATTGAAGCTACGCGACTAGA	954
wheat	ycf3	TCAATCCGAAGGAAATATGCGGAAGCTTTGCAAAATTTATTGAAGCTACGCGACTAGA *****	950
WT	ycf3	AATCGATCCCTATGATCGAAGTTATATACTCTATAACATAGGCCTTATACACACAAGCAA	1013
CL3	ycf3	AATCGATCCCTATGATCGAAGTTATATACTCTATAACATAGGCCTTATACACACAAGCAA	1014
wheat	ycf3	AATCGATCCCTATGATCGAAGTTATATACTCTATAACATAGGCCTTATACACACAAGCAA *****	1010
WT	ycf3	TGGAGAGCATACAAGGCTTTGGAATATTATTTCCGGGCACTAGAACGAAAACCCCTTCTT	1073
CL3	ycf3	TGGAGAGCATACAAGGCTTTGGAATATTATTTCCGGGCACTAGAACGAAAACCCCTTCTT	1074

wheat	ycf3	TGGAGAGCATACAAGGCTTTGGAATATTATTTCCGGCACTAGAACGAAACCCCTTCTT	1070

WT	ycf3	ACCGCAAGCTTTTAATAATATGGCCGTGATCTGTCAATAC GTGCGACTATCTCCACTATA	1133
CL3	ycf3	ACCGCAAGCTTTTAATAATATGGCCGTGATCTGTCAATAC GTGCGACTATCTCCACTATA	1134
wheat	ycf3	ACCGCAAGCTTTTAATAATATGGCCGTGATCTGTCAATAC GTGCGACTATCTCCACTATA	1130

WT	ycf3	GAAAGACAAAAAA-GAGAGGATCAAATTTTCTAGTAATACTGGAAAAA-GGGCTTTC	1191
CL3	ycf3	GAAAGACAAAAAA-GAGAGGATCAAATTTTCTAGTAATACTGGAAAAA-GGGCTTTC	1192
wheat	ycf3	GAAAGAAAAAAAAGAGAGGATCAAATTTTCTAGTAATACTAGAAAAAAGGGCTTTC	1190

WT	ycf3	TACATAGGGATCGTAAAAACAACGATTTTTCCCTATCAGCTGTAGGAAGGAAGGACACTT	1251
CL3	ycf3	TACATAGGGATCGTAAAAACAACGATTTTTCCCTATCAGCTGTAGGAAGGAAGGACACTT	1252
wheat	ycf3	TACATAGGGATCGTAAAAACAACGATTTTTCCCTATCAGCTGTAGGAAGGAAGGACACTT	1250

WT	ycf3	CACGAGAATCAAAAAACGAAGAAAGTATGGCCTATACTACTCTATGGATAAAGTTTC	1311
CL3	ycf3	CACGAGAATCAAAAAACGAAGAAAGTATGGCCTATACTACTCTATGGATAAAGTTTC	1312
wheat	ycf3	CACGAGAATCAAAAAACGAAGAAAGTATGGCCTATACTACTCTATGGATAAAGTTTC	1310

WT	ycf3	TCAAATTTGATAGAGAAAGCACCCTAAAGATCAATTAGTGAGCGACTGGGTCGATACAAC	1371
CL3	ycf3	TCAAATTTGATAGAGAAAGCACCCTAAAGATCAATTAGTGAGCGACTGGGTCGATACAAC	1372
wheat	ycf3	TCAAATTTGATAGAGAAAGCACCCTAAAGATCAATTAGTGAGCGACTGGGTCGATACAAC	1370

WT	ycf3	AAAAAAACTGCTTACTTATCCCATGATATGGGGCAAATTTAGGAATCCGCTTATGTAA	1431
CL3	ycf3	AAAAAAACTGCTTACTTATCCCATGATATGGGGCAAATTTAGGAATCCGCTTATGTAA	1432
wheat	ycf3	AAAAAAACTGCTTACTTATCCCATGATATGGGGCAAATTTAGGAATCCGCTTATGTAA	1430

WT	ycf3	TAGAGCCGATCCACTAAGGGATTAAGCAGCGGTGTAGTATCAGATCCCAAAGATAGTAAG	1491
CL3	ycf3	TAGAGCCGATCCACTAAGGGATTAAGCAGCGGTGTAGTATCAGATCCCAAAGATAGTAAG	1492
wheat	ycf3	TAGAGCCGATCCACTAAGGGATTAAGCAGCGGTGTAGTATCAGATCCCAAAGATAGTAAG	1490

WT	ycf3	TTCTTTTTCTTTCTTATGG-----AAAAAAGTCTTTTTCAAGGATTCTATAGAGATTTT	1546
CL3	ycf3	TTCTTTTTCTTTCTTATGG-----AAAAAAGTCTTTTTCAAGGATTCTATAGAGATTTT	1547
wheat	ycf3	TTCTTTTTCTTTCTTATGGTATGGAAAAAAGTCTTTTTCAAGGATTCTATAGAGATTTT	1550

WT	ycf3	ATATATGAAACCGGGATAGTTACCTTTTCAGAAAAATTTGAACGAAGGCTCTATATCTATCT	1606
CL3	ycf3	ATATATGAAACCGGGATAGTTACCTTTTCAGAAAAATTTGAACGAAGGCTCTATATCTATCT	1607
wheat	ycf3	ATATATGAAACCGGGATAGTTACCTTTTCAGAAAAATTTGAACGAAGGCTCTATATCTATCT	1610

WT	ycf3	ATGCTTCATTCTTCTGAAGGTGGGAAAAAAGATCAAATAATTATTGAGAAAAATTAGGG	1666
CL3	ycf3	ATGCTTCATTCTTCTGAAGGTGGGAAAAAAGATCAAATAATTATTGAGAAAAATTAGGG	1667
wheat	ycf3	ATGCTTCATTCTTCTGAAGGTGGGAAAAAAGATCAAATAATTATTGATAAAAATTAGGG	1670

WT	ycf3	TTTGAAACTTAGGTAATTAATTTCTTCTGCTTA-ACACAAGAACAATTTGGATCGATTTT	1725
CL3	ycf3	TTTGAAACTTAGGTAATTAATTTCTTCTGCTTA-ACACAAGAACAATTTGGATCGATTTT	1726
wheat	ycf3	TTTGAAACTTAGGTAATTAATTTCTTCTGCTTAGACCAAGAACAATTTGGATCGATTTT	1730

WT	ycf3	TGATAAATCGAATTCAGTTAAGATAGGGGAAATTAAGATAGCAATTTCTGAGCCGATGA	1785
CL3	ycf3	TGATAAATCGAATTCAGTTAAGATAGGGGAAATTAAGATAGCAATTTCTGAGCCGATGA	1786
wheat	ycf3	TGATAAATCGAATTCAGTTAAGATAGGGGAAATTCAGATAGCAATTTCTGAGCCGATGA	1790

WT	ycf3	GGTAGGAACTCTCAAGTACGGTTCTAAGGGAAGGAACTGCCTATTTCCGAC CGAGGAGAA	1845
CL3	ycf3	GGTAGGAACTCTCAAGTACGGTTCTAAGGGAAGGAACTGCCTATTTCCGAC CGAGGAGAA	1846
wheat	ycf3	GGTAGGAACTCTCAAGTACGGTTCTAAGGGAAGGAACTTCTATTTCCGAC CGAGGAGAA	1850

WT	ycf3	CAGGCCATTCTAGAGGGTGATTCGGAAATTCGGGAAGCTTGGTTTGATCAAGCTGCTGAA	1905
CL3	ycf3	CAGGCCATTCTAGAGGGTGATTCGGAAATTCGGGAAGCTTGGTTTGATCAAGCTGCTGAA	1906
wheat	ycf3	CAGGCCATTCTACAGGGTGATTCGGAAATTCGGGAAGCTTGGTTTGATCAAGCTGCTGAA	1910

WT	ycf3	TATTGGAAACAAGCTATAGCGCTTACTCCGGGAAATTTATATTGAAGCACAAAACCTGGTTG	1965
CL3	ycf3	TATTGGAAACAAGCTATAGCGCTTACTCCGGGAAATTTATATTGAAGCACAAAACCTGGTTG	1966
wheat	ycf3	TATTGGAAACAAGCTATAGCGCTTACTCCGGGAAATTTATATTGAAGCACAGAAGCTGGTTG	1970

WT	ycf3	AAGATTACGAAGCGCTTTGAATTTGAATAA	1995
CL3	ycf3	AAGATTACGAAGCGCTTTGAATTTGAATAA	1996
wheat	ycf3	AAGATTACGAAGCGCTTTGAATTTGAATAA	2000

Supplemental Figure S4. DNA sequence alignment of *ycf3* gene from WT, CL3 and wheat. Exons are shown in yellow, mutations are highlighted in red. ∇: editing site C→T

WT ycf3 DNA	ATGCCTAGATCCCCTGTAATAATGGAAATTTTCATTGATAAGACCTTCTCAATTATAGCCAA	59
CL3 ycf3 cDNA	ATGCCTAGATCCCCTGTAATAATGGAAATTTTCATTGATAAGACCTTCTCAATTATAGCCAA	59

WT ycf3 DNA	TATTTTATTGCGAATAATTCGACAACCTCAGGAGAAAAAAGGCATTTACTTATTATAG	119
CL3 ycf3 cDNA	TATTTTATTGCGAATAATTCGACAACCTCAGGAGAAAAAAGGCATTTACTTATTATAG	119

WT ycf3 DNA	AGATG GTGCGATTTGACTCTTTTTTTTTTTT GCTTTTTTTTAGACCTACCTATACCTCAG	178
CL3 ycf3 cDNA	AGATG GTGCGATTTGACTCTTTTTTTTTTTT GCTTTTTTTTAGACCTACCTATACCTCAG	179

WT ycf3 DNA	TCTTAGGAAAAAGAAAAGGGGTGGCATAGAGAGAACCAAAATTTGTAAGCAAGCAAACC	238
CL3 ycf3 cDNA	TCTTAGGAAAAAGAAAAGGGGTGGCATAGAGAGAACCAAAATTTGTAAGCAAGCAAACC	239

WT ycf3 DNA	CACGCTTCGGGAAGGTGAGGCGAACTAACAAATTCCTTCCGTCGTGTATCCTCGATTGATG	298
CL3 ycf3 cDNA	CACGCTTCGGGAAGGTGAGGCGAACTAACAAATTCCTTCCGTCGTGTATCCTCGATTGATG	299

WT ycf3 DNA	CGGCTTCAGATACTTCAATTGTAGATTTGAGTATTGAGCGAAAGGTTACACCTACAGGAT	358
CL3 ycf3 cDNA	CGGCTTCAGATACTTCAATTGTAGATTTGAGTATTGAGCGAAAGGTTACACCTACAGGAT	359

WT ycf3 DNA	ATGGTATGGTATGGATTACAGGCCACTCTATTAGTATCCGTAGGCAGCATAGGGGAGAAA	418
CL3 ycf3 cDNA	ATGGTATGGTATGGATTACAGGCCACTCTATTAGTATCCGTAGGCAGCATAGGGGAGAAA	419

WT ycf3 DNA	AGCACTACCTAGAAATAGGAATCAACAAGAGAAAACTTTGGTAGAAATTACCCCTTT	478
CL3 ycf3 cDNA	AGCACTACCTAGAAATAGGAATCAACAAGAGAAAACTTTGGTAGAAATTACCCCTTT	479

WT ycf3 DNA	CCTGATCGGTATCAGGGCTGGGAAGAATGGTTGGGATAACAACAACCA CAGGTTTGTA	538
CL3 ycf3 cDNA	CCTGATCGGTATCAGGGCTGGGAAGAATGGTTGGGATAACAACAACCA CAGGTTTGTA	539

WT ycf3 DNA	CTTTGGATACCCCTATAACCATCAAAGATCGTTGAAGTAGCTAATTCCTCTAAATAGGAG	598
CL3 ycf3 cDNA	CTTTGGATACCCCTATAACCATCAAAGATCGTTGAAGTAGCTAATTCCTCTAAATAGGAG	599

WT ycf3 DNA	GCGTTGAGAACAAGAAATATTGGAGCTATCGTTTTCTCTAGCATTAAATAGAATTCAT	658
CL3 ycf3 cDNA	GCGTTGAGAACAAGAAATATTGGAGCTATCGTTTTCTCTAGCATTAAATAGAATTCAT	659

WT ycf3 DNA	TGGTGTTAAGAAAAACCTCTTGTGGGAAGGTTGGCTAGAGATTTCTTGGAAAAATACCAG	718
CL3 ycf3 cDNA	TGGTGTTAAGAAAAACCTCTTGTGGGAAGGTTGGCTAGAGATTTCTTGGAAAAATACCAG	719

WT ycf3 DNA	CCCTTTTCGGTTCATAATGAGACGGGACTAATTCATTTTGATTCTATAGATTAAGATTA	778
CL3 ycf3 cDNA	CCCTTTTCGGTTCATAATGAGACGGGACTAATTCATTTTGATTCTATAGATTAAGATTA	779

WT ycf3 DNA	TTTCGCTTAGTACTATTATGTACAGAAGGGAGGAGCCGTATGAGATGAAAACCTCATGTA	838
CL3 ycf3 cDNA	TTTCGCTTAGTACTATTATGTACAGAAGGGAGGAGCCGTATGAGATGAAAACCTCATGTA	839

WT ycf3 DNA	CGGTTTGGAAACGGAGATTTTTTGAATAGAATGAACGCCGTAAC GGATGTTGGCTCAAT	898
CL3 ycf3 cDNA	CGGTTTGGAAACGGAGATTTTTTGAATAGAATGAACGCCGTAAC GGATGTTGGCTCAAT	899

WT ycf3 DNA	CCGAAGGAAATATGCGGAAGCTTTGCAAAATTTATATGAAGCTA CCGACTAGAAATCG	958
CL3 ycf3 cDNA	CCGAAGGAAATATGCGGAAGCTTTGCAAAATTTATATGAAGCTA CCGACTAGAAATCG	959

WT ycf3 DNA	ATCCCTATGATCGAAGTTATATACTCTATAACATAGGCCTTATACACACAAGCAATGGAG	1018
CL3 ycf3 cDNA	ATCCCTATGATCGAAGTTATATACTCTATAACATAGGCCTTATACACACAAGCAATGGAG	1019

WT ycf3 DNA	AGCATACAAAGGCTTTGGAATATATTCCGGGCACTAGAACGAAACCCCTTCTTACCCG	1078
CL3 ycf3 cDNA	AGCATACAAAGGCTTTGGAATATATTCCGGGCACTAGAACGAAACCCCTTCTTACCCG	1079

WT ycf3 DNA	AAGCTTTTAATAATATGGCCGTGATCTGTCTATTAC GTGCGACTATCT-CCACTATAGAAA	1137
CL3 ycf3 cDNA	AAGCTTTTAATAATATGGCCGTGATCTGTCTATTAC CGAGGAGAACAGCCATTCTAGG --	1137

WT ycf3 DNA	GACAAAAAAGAGAGGATCAAATTTCTAGTAAATACTGGAAAAAGGGCTTTCTACATA	1197

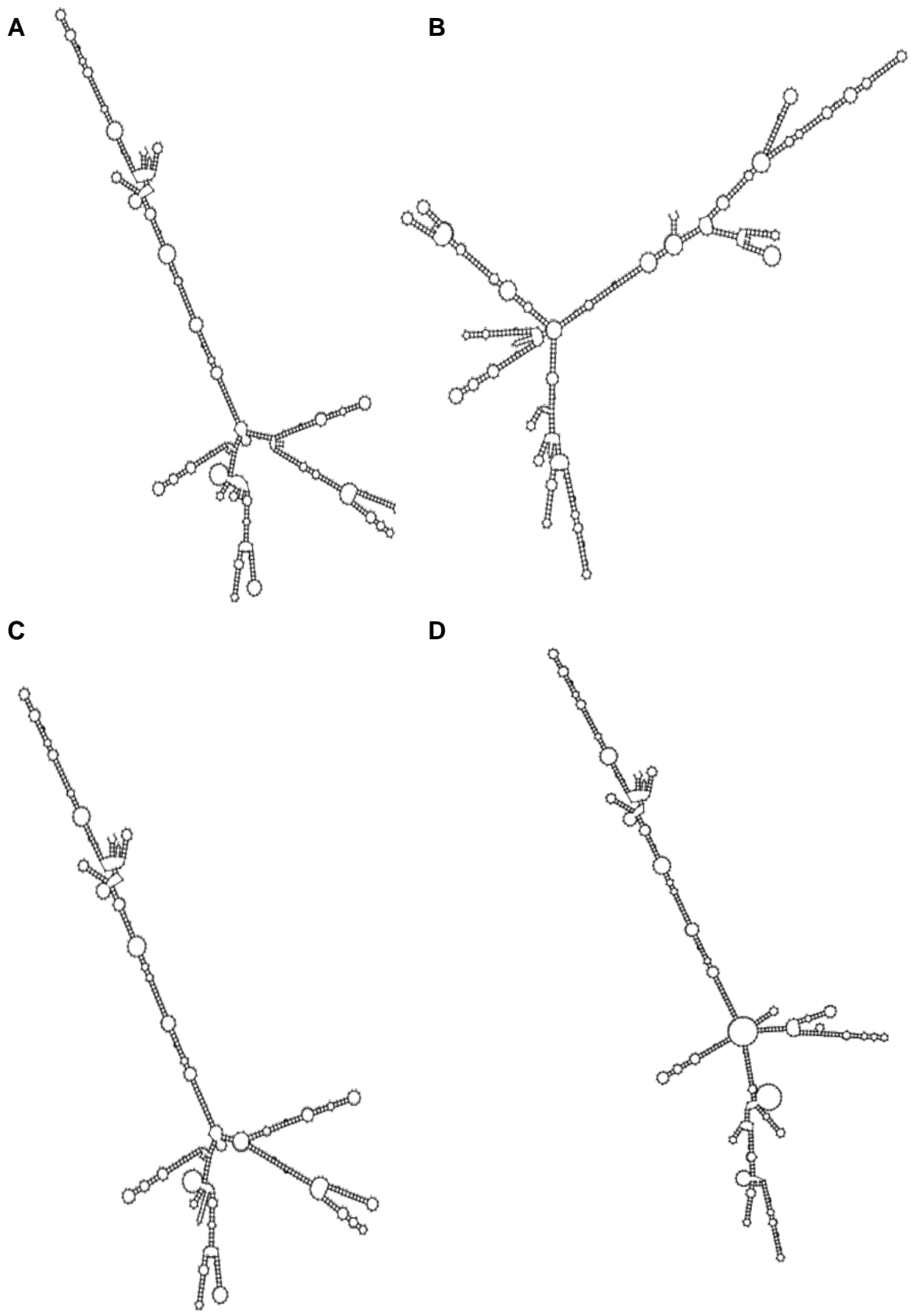
exon 1

intron 1

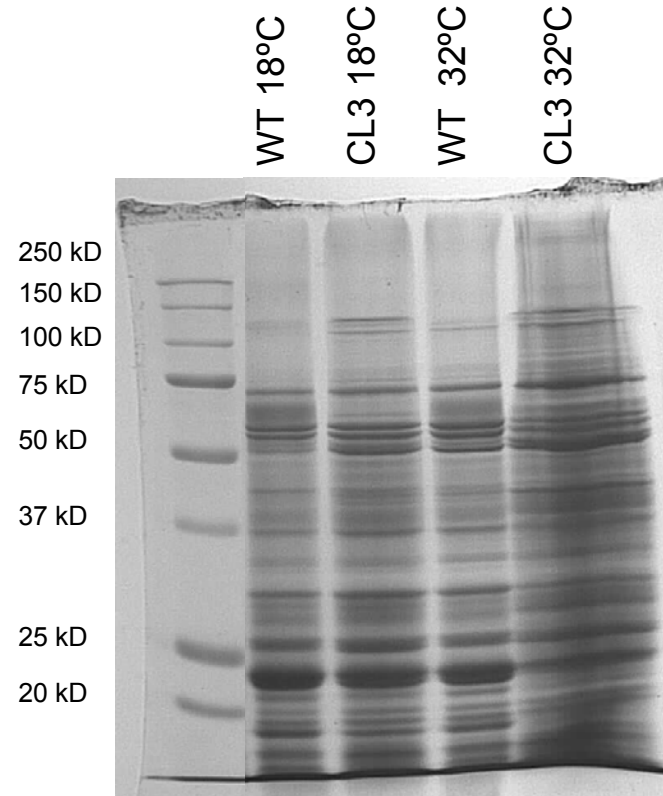
exon 2

CL3 ycf3 cDNA	-----GGTGTTCGGAAATTGCGGAAGCTTGGTTGATCAAGCTGCTGAATATT	1187	
	* *		
WT ycf3 DNA	GGGATCGTAAAAACAACGATTTTCCCTATCAGCTGTAGGAAGGAAGGACACTTCACGAG	1257	exon 3
CL3 ycf3 cDNA	GGAAACA-AGCTATAGCGCTTACTCCGGGA-AATTATATTGAAGCACAAAAC-----	1237	
	** *		

Supplemental Figure S5. Sequence alignment of *ycf3* gene DNA from WT and CL3 intron 1-containing *ycf3* cDNA. Exons 1 and 2 are shown in yellow, mutations are highlighted in red, exon 3 is shown green and the editing site is highlighted in blue.



S. Figure S6. RNA FOLD prediction of *ycf3* intron 1: A, WT 18°C; B, CL3 18°C; C, WT 32°C; D, CL3 32°C (The RNAfold web server, University of Vienna).



S. Figure S7. SDS-PAGE gel stained with Coomassie blue corresponding to immunoblot against Ycf3 protein from Figure 7. Thylakoid protein extracts from WT and CL3 seedlings were loaded on a chlorophyll basis of 5 μg . Thylakoid homogenates were extracted from seedlings of 6 days after germination grown at 18°C or at 32°C under a mixture of fluorescent and incandescent light (100 $\mu\text{mol photons m}^{-2} \text{s}^{-1}$).